MEASUREMENT OF LENGTH AND EULER CHARACTERISTIC IN 3D IMAGES

JIŘÍ JANÁČEK*, IVAN SAXL**

*Institute of Physiology, ASCR, Praha, Czech Republic (janacek@biomed.cas.cz),
**Mathematical Institute, ASCR, Praha, Czech Republic (saxl@math.cas.cz)

Abstract Efficient procedures for automatic measurements of length and Euler characteristic in 3D images are presented. The effect of background noise on the measurement of length and Euler characteristic of a fibrous structure is estimated.

Keywords: length, Euler characteristic, 3D, noise, anisotropy

1 Introduction

The aim of the paper is a simple and efficient implementation of measurements in 3D binary image. Wrong segmentation or insufficient image resolution, anisotropy of the measured structure and contamination by image noise artefacts may bias results of the measurements of a real sample. We will discuss the precision of estimates of length of anisotropic structures in order to design estimators of length more robust with respect to the anisotropy bias. The effect of contamination of the image by noise artefacts will be estimated using geometry of Gaussian random fields.

2 Methods

2.1 Intrinsic volumes

The intrinsic volume [7] can be defined for a convex set C in $\boldsymbol{R}^d$ as the integral of a j-dimensional measure of its j-dimensional projection averaged over all possible projection directions (the generalized Cauchy formula). The intrinsic volume of a union of convex sets is defined additively. The intrinsic volume is monotone, additive, motion invariant and homogeneous of order j and is normalised so that the following relations to the Lebesgue measure λ^d, the Hausdorff measure H and the Euler characteristic χ hold:

$$V_d(C) = \lambda^d(C),\ V_{d-1}(C) = H^{d-1}(\delta C)/2,\ V_1(C) = H^1(C),\ V_0(C) = \chi(C).$$

In 2D, $V_2(C) = S(C)$ is the area of C and $2V_1(C) = p(C)$ is the perimeter of C. In 3D, $2V_2(C) = S(C)$ is the surface area of C and $V_1(C) = L(C)$ is the "length" (in fact, twice the mean width) of C.

Crofton relation holds for sections of C by k-flats $F_k = L_k + x$ ($L_k^\perp$ is the linear $(d\text{-}k)$-subspace orthogonal to the linear k-subspace L_k and G_{dk} is the Grassmann manifold):

$$\int_{G_{dk}} \int_{L_k^\perp} V_j\left(C \cap (L_k + x)\right) d\lambda^{d-k}(x)\, d\mu(L_k) = c_{djk} V_{d+j-k}(C) \tag{1}$$

with the coefficients

$$c_{djk} = \gamma_k^d \gamma_{d+j-k}^d / \gamma_j^d,\ \gamma_i^d = (\kappa_i i!)/(\kappa_d d!),\ \kappa_d = \pi^{d/2} \Gamma(d/2+1)^{-1},$$

where κ_d is the d-dimensional volume of a unit ball in d-dimensional space $\boldsymbol{R}^d$.

Important values of the coefficient are $c_{201} = 2/\pi$ in 2D and $c_{302} = c_{301} = 1/2$ in 3D.

2.2 Systematic sampling of directions in the Crofton relation

The Crofton relation makes possible to estimate length of an object C by an isotropic random choice of the direction in $\boldsymbol{R}^d$ and formula

$$estV_1(C) = \frac{1}{c_{d01}} \int_{L_{d-1}^{\perp}} V_0\left(C \cap \left(L_{d-1} + x\right)\right) d\lambda^1(x),$$

where $L_{d-1}^{\perp}$ corresponds to the chosen direction. Let us call the integral in the above formula the (total) projection of C onto $L_{d-1}^{\perp}$ [6]. The precision of the estimator may be poor if we measure strongly anisotropic objects. Selecting the directions in a systematic way and combining the information from the partial estimators to the single estimator by taking their (weighted) average we can substantially decrease the variance of the estimator by antithetic effect [4]. The variance of the systematic estimator of the length of a line segment in the d-dimensional space can be calculated from the correlation coefficient of the projections into two directions with angle ψ:

$$r_d(\psi) = \frac{2}{c_{d01}^2 d\pi}\left(\sin\psi + \left(\frac{\pi}{2} - \psi\right)\cdot\cos\psi\right) - 1 \qquad (2)$$

[1]. The coefficient of variation (CV) of the estimates using a single isotropically randomly oriented direction may be as high as $1/\sqrt{3} \cong 0.58$ in 3D. If we use the average of estimates with three perpendicular directions in 3D, the CV is at most $\sqrt{16/\pi - 5}/3 \cong 0.102$. The CV for the rose of directions of normals to unbounded cylindrical surface that is approximately 0.037 according to [4] has the exact value

$$\sqrt{\frac{32}{9\pi^2}\left(1 + \frac{1}{\pi}\left(K^2 + \frac{3\pi^2}{4K^2}\right)\right) - 1}, \quad \text{where } K = \frac{\Gamma(1/4)^2}{4\sqrt{\pi}},$$

as we calculated using the identities between generalized hypergeometric functions.

Weights w_i of the estimator with the minimal value of variation coefficient for a set of directions and an actual object with isotropic random orientation can be calculated using the inverse $C^{-1} = D = (d_{ij})$ of the covariance matrix $C = (c_{ij})$ of the object projections:

$$w_i = \sum_j d_{ij} \Big/ \sum_{j,k} d_{jk} \qquad (3)$$

[2]. A sufficiently general choice of the object is the line segment, as it represents the worst case from the point of view of variance of the estimator and as it allows an explicit calculation of the covariances of the projections (2).

2.3 Estimates of the length and of the Euler characteristics using binary images

Digital images are the lattices of spatial elements (spels, *i.e.* pixels in 2D and voxels in 3D) with assigned numbers or vectors. Binary image consists of spels with values 0 and 1 indicating whether the spel belongs to the background or to the objects (foreground), respectively. If we want to use the images for estimation of the volume of objects under study we must know the spatial arrangement of spels (area or volume per spel). For estimation of the Euler characteristic of the objects by calculation of the Euler characteristic of the digitized objects we must define the adjacency (neighbouring relation) of the spels in the binary image and for estimation of the other intrinsic volumes

by a digital counterpart of the Crofton relation (1) we must select sets of principal digital affine subspaces with spel adjacencies [6].

Let the spels of the $\boldsymbol{R}^d$ image be arranged in an orthogonal lattice with regular spacings s_1, s_2, …, s_d (calibration constants) between the centres of spels in each dimension, and indexed by multiindices from the set $\{1,2,\ldots,n_1\}\times$ $\times\{1,2,\ldots,n_2\}\times\ldots\times\{1,2,\ldots,n_d\}$ and let the spel adjacency be either $2d$-adjacency (neighbouring spels are those that differ by one step in one coordinate only: 2-adjacency in 1D, 4-adjacency in 2D, 6-adjacency in 3D) or $(3^d\text{-}1)$-adjacency (neighbouring spels differ at most by one step in each coordinate: 2-adjacency in 1D, 8-adjacency in 2D, 26-adjacency in 3D).

For example, there are two basic textural characteristics in 1D. The total length (1-dimensional volume) we calculate by multiplying the number the foreground spels by the calibration constant. The number $\hat{\chi}_2$ of intervals ($\hat{\chi}_2$ denotes an estimator of χ, the Euler characteristic of the object under study) we calculate by counting the rightmost spels of the intervals (f is the function attributing the binary value to the spels, $\wedge$, $\vee$ and — are the logical AND, OR and NOT, resp., and n stands for n_1):

$$\hat{\chi}_2 = \sum_{i=1}^{n-1} f(i) - f(i) \wedge f(i+1) = \sum_{i=1}^{n-1} f(i) \wedge \overline{f(i+1)}. \tag{4a}$$

Alternatively the leftmost points can be counted, which yields

$$\hat{\chi}_2 = \sum_{i=1}^{n-1} f(i) \vee f(i+1) - f(i) = \sum_{i=1}^{n-1} \overline{f(i)} \wedge f(i+1). \tag{4b}$$

The two numbers are different if the value of just one of the boundary spels is 1, which can be corrected by subtracting the value of $0.5(f(1)-f(n))$ from the first formula and adding it to the second one. Similar boundary corrections can be applied to all the estimators used in this section to diminish their anisotropic behaviour.

The d-dimensional volume occupied by the foreground spels can be calculated by adding their volumes. A formula for the Euler characteristic of binary images with orthogonal lattice in $\boldsymbol{R}^d$ can be defined by induction. This formula makes possible an efficient implementation of the measurement algorithm with the spels coded by the bits of integral data types and the formulas implemented with the bit shift and logical operators. We can start the definition from dimension 0, where the image has single binary spel and the connectivity is 0 or 1, equal to the spel value. Let $f(i,\bullet)$ be the $(d\text{-}1)$-dimensional slice at the position i through the image. Then the Euler characteristic of the d-dimensional image can be calculated from the Euler characteristic of $(d\text{-}1)$-dimensional slices [5]:

$$\hat{\chi}_{2d} = \sum_{i=1}^{n_d-1} \hat{\chi}_{2(d-1)}(f(i,\bullet)) - \hat{\chi}_{2(d-1)}(f(i,\bullet) \wedge f(i+1,\bullet)), \tag{5a}$$

$$\hat{\chi}_{3^d-1} = \sum_{i=1}^{n_d-1} \hat{\chi}_{3^{d-1}-1}(f(i,\bullet) \vee f(i+1,\bullet)) - \hat{\chi}_{3^{d-1}-1}(f(i,\bullet)). \tag{5b}$$

The first induction step yields the 1D formulas (4a,b). The formulas for $\hat{\chi}_4$, $\hat{\chi}_8$ in 2D and for $\hat{\chi}_6$ in 3D are equivalent to the currently used methods [3,6]. Calculations with other adjacencies in the orthogonal lattices, *e.g.* 6-adjacency in 2D (4-adjacency plus one of diagonal configurations), or calculations in nonorthogonal lattices as is triangular lattice in 2D [6] can also be easily implemented.

The length in 3D can be estimated by digital version of the Crofton relations (1) using planar sections in three perpendicular principal directions:

$$\hat{L}=\frac{2}{3}\left(s_1\sum_{i=1}^{n_1}\hat{\chi}\left(f(\bullet,\bullet,i)\right)+s_2\sum_{i=1}^{n_2}\hat{\chi}\left(f(\bullet,i,\bullet)\right)+s_3\sum_{i=1}^{n_3}\hat{\chi}\left(f(i,\bullet,\bullet)\right)\right), \tag{6}$$

where *e.g.* the 6-adjacent estimator is used for calculation of the 2D connectivity number in the parallel section planes. In the case of a highly anisotropic object or of an object with non-random orientation, *e.g.* aligned along the edges of the 3D image, it is preferable to estimate the length by weighted average of estimates using Euler characteristics of intersections of the object with the parallel planes defined by the triplets of the 26-neighbours (their normals are the directions connecting the neighbours of the dual grid). As the directions are not evenly distributed on the hemisphere in the case of an orthogonal lattice, especially if the lattice is not cubic, some weighting of the results from partial estimators, *e.g.* that one recommended in the formula (3), is important for the compensation of the effect of anisotropy.

2.4 Intrinsic volumes of Gaussian excursion sets

Smoothing the *d*-dimensional image with an uncorrelated Gaussian noise by the Gaussian kernel with standard deviation ρ results in the smooth Gaussian field with Gaussian covariance function *R*:

$$X(x)\sim N(\mu,\sigma),\qquad R(x)=\exp\left(-|\eta x|^2/2\right),$$

where $\eta=\left(\sqrt{2}\rho\right)^{-1}$. The excursion set $U(u)$ and the spatial density of *j*-th intrinsic volume V_j' are

$$U(u)=\{x\mid X(x)\geq u\},\qquad V_j'=\lim_{r\to\infty}\frac{EV_j\left(B_{0r}\cap U(u)\right)}{V_d\left(B_{0r}\right)},$$

where B_{0r} is the ball of radius *r* centred in the origin.

Then (with the notation $H_n(t)$ for the Hermite function) [8]

$$V_{d-j}'\left(U(u)\right)=c_{d0j}^{-1}\eta^j(2\pi)^{-\frac{j+1}{2}}H_{j-1}\left(\frac{u-\mu}{\sigma}\right),\quad H_n(t)=(-1)^n\frac{d^n\exp\left(-t^2/2\right)}{dt^n}. \tag{7}$$

2.5 Random geometric graph

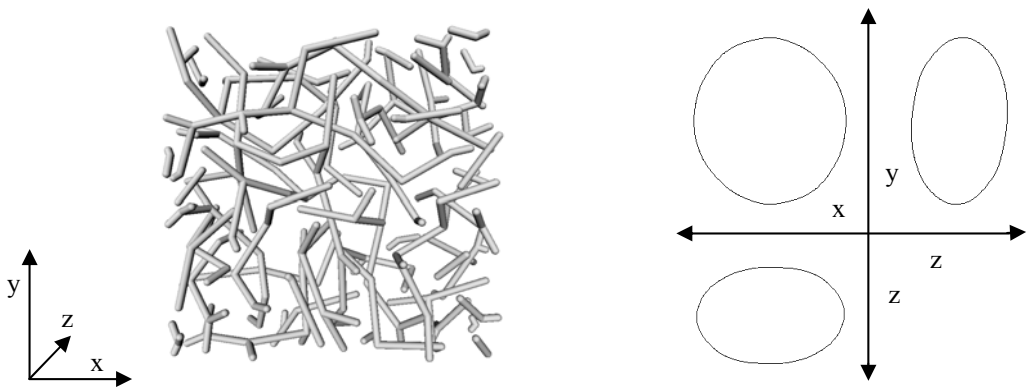

Fig. 1: Realization of the random geometric graph (left), the segments are visualized as thin cylinders joined by balls. Projections of the Steiner body of the graph (right).

The model was designed to generate structures resembling microscopic samples of blood capillaries in animal brain. The simulation window was 256 units wide, 256 units high and 128 units thick. In the first step the vertices of the graph were generated as points of

the simple sequentially inhibited random process (SSI) with distance of inhibition 15 units, then the segments of length less than 30 units connecting the points were sequentially generated under conditions: a) number of segments adjacent to a vertex is less or equal to 3, b) the segments with a common vertex form an obtuse angle, c) the distance of the middle point of the segment from the points and the middle points of the already generated segments is greater than 10 units. The border with horizontal thickness 64 units and the vertical thickness 32 units was removed. Finally the segments were contracted in the z-direction by factor 2.

The image of a realization of the model is in Figure 1. The projections of the Steiner body of the segments were calculated as the Minkowski sums of the respective projections of the segments.

3 Results

3.1 Length and Euler characteristic

100 realizations of the random graph, described in the section 2.5, were generated. The length was calculated by summation of lengths of the segments, the average length density was $6.68 \cdot 10^{-3}$ with the standard deviation (SD) $2 \cdot 10^{-4}$. The Euler characteristic was calculated as number of vertices of degree 1 minus the number of vertices of degree 3 dividing the result by 2. The average Euler characteristic density was $1.03 \cdot 10^{-5}$, SD = $7.1 \cdot 10^{-6}$.

The binary images of the graphs with voxels in unit cubic lattice were drawn and dilated by cubooctahedral structural element with 19 voxels. The Euler characteristic was estimated as the mean of the 6-connected estimate (5a) and the 26-connected estimate (5b) (the mean provides some boundary correction), the average bias of the estimated Euler characteristic density was $-7.6 \cdot 10^{-8}$, SD = $4.64 \cdot 10^{-6}$. The length was estimated by formula (6), the average bias of the estimated length density was $-8.92 \cdot 10^{-4}$, SD = $1 \cdot 10^{-4}$.

3.2 Measurements in presence of noise

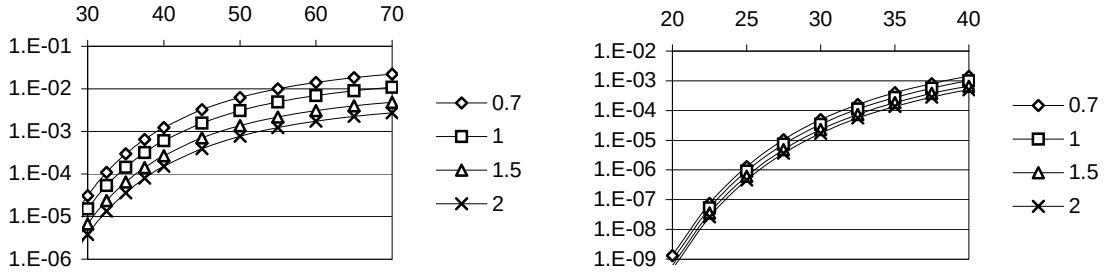

Fig. 2: The length density (left, y-axe) and Euler characteristic density (right, y-axe) of the excursion set U(128) of the Gaussian field with standard deviation (σ, x-axes) for various degree of smoothness (ρ) by formula (7).

Let the realizations of the model described in Section 2.5 be drawn by thick lines with full contrast equal to 256 levels. Supposing the volume of the lines is negligible, we can see on the Figure 2, showing the graphs of length density and Euler characteristic density of the excursion set $U(128)$ of Gaussian random fields, that for a moderate degree of smoothing $\rho = 1$ and acceptable bias $1 \cdot 10^{-4}$ for the length measurement the maximal level of noise is about $\sigma = 35$, while for the Euler characteristic measurement with the same

degree of smoothing and acceptable bias $1 \cdot 10^{-6}$ the maximal level of noise is about $\sigma = 25$.

To confirm the validity of the predictions from the continuous model described in 2.4 for discrete images the binary images of realizations of the random graphs were converted to floating point images with contrast 384, contaminated by uncorrelated noise with standard deviations 0, 105, 145, 185 and smoothed by Gaussian filter with standard deviation $\rho = 1$. These values were chosen empirically in order to obtain the discrete Gaussian random field with standard deviations $\sigma = 0$, 25, 35, 45 after smoothing by Gaussian filter with standard deviation $\rho = 1$.

The average bias of length density measurement at noise with $\sigma = 35$ was $5.15 \cdot 10^{-4}$, SD = $4 \cdot 10^{-5}$, and $2.17 \cdot 10^{-3}$, SD = $9.7 \cdot 10^{-5}$ at $\sigma = 45$. The average bias of Euler characteristic density measurement at noise with $\sigma = 25$ was $-1.5 \cdot 10^{-6}$, SD = $2.3 \cdot 10^{-6}$, and $3.64 \cdot 10^{-5}$, SD = $7.9 \cdot 10^{-6}$, at $\sigma = 35$.

4 Conclusion

Measurement of Euler characteristic and length in 3D can be implemented using only bit-shifts and logical operations on integers. The maximal level of noise in the source image that do not disturb measurement of length or Euler characteristic can be estimated from the theory of Gaussian random fields. The estimate of the Euler characteristic is more sensitive to the image noise.

Acknowledgement

The study was supported by the Academy of Sciences of the Czech Republic (Grants A100110502 and AV0Z 50110509).

References

[1] Janáček, J.: *Errors of spatial grids estimators of volume and surface area,* Acta Stereologica 18 (1999), 389-396.

[2] Janáček, J.: *Estimating length and surface area by systematic projections,* Image Analysis and Stereology 20 (2001), Supplement 1, CD-ROM, 89-94.

[3] Lee, C.N., Poston, T., Rosenfeld, A.: *Winding and Euler numbers for 2D and 3D digital images*, CVGIP: Graphical Models Image Processing 53 (1991), 522-537.

[4] Mattfeldt, T., Mobius, H.-J., Mall, G.: *Orthogonal triplet probes: an efficient method for unbiased estimation of length and surface of objects with unknown orientation in space*. J. Microsc. 139 (1985), 279-289.

[5] Nagel, W., Ohser, J., Pischang, K.: *An integral-geometric approach for the Euler-Poincaré characteristic of spatial images.* J. Microsc. 198 (2000), 54-62.

[6] Serra, J.: *Image Analysis and Mathematical Morphology*. Academic Press, London 1982.

[7] Weil, W.: *Integral geometry, stochastic geometry, and stereology.* Acta Stereologica 8 (1989), 65-76.

[8] Worsley, K.J.: *Estimating the number of peaks in a random field using the Hadwiger characteristic of excursion sets, with applications to medical images.* Annals of Statistics 23 (1995), 640-669.